doi:10.3788/gzxb20174607.0706007

用于液压传感的双芯光子晶体光纤

李海涛,王晓亮,折丽娟,陈达如

(浙江师范大学 数理与信息工程学院 光学信息研究所,浙江 金华 321004)

摘 要:采用全矢量有限元方法进行光纤设计优化,得到横截面上失去两层空气洞的双芯光子晶体光纤,可用于液压传感.优化的双芯光子晶体光纤的模场半径和数值孔径与单模光纤基本一致,在优化的双芯光子晶体光纤和单模光纤之间有一个相对较低的熔接损耗.计算结果表明由模场半径和数值孔径导致的不匹配造成的总共损耗可低至 0.026 dB,低于传统光子晶体光纤和单模光纤 0.1 dB 的直接熔接损耗.对基于 20 cm 双芯光子晶体光纤的液压传感器的性能进行研究,结果表明在 0~500 MPa 量程内的灵敏度为 -1.6 pm/MPa.

关键词:光纤光学;液压传感;有限元方法;双芯光子晶体光纤;模场半径;数值孔径

中图分类号:O436 **文献标识码**:A **文章编号**:1004-4213(2017)07-0706007-5

Dual-core Photonic Crystal Fiber for Hydrostatic Pressure Sensing

LI Hai-tao, WANG Xiao-liang, SHE Li-juan, CHEN Da-ru

(*Institute of Optical Information, College of Mathematics and Information Engineering, Zhejiang Normal University, Jinhua, Zhejiang* 321004, *China*)

Abstract: By a full-vector finite-element method, the dual-core photonic crystal fiber for hydrostatic pressure sensing with two layers of air holes in the cross-section missed was designed and optimized, The mode field radius and numerical aperture of the optimized dual-core photonic crystal fiber are almost the same as that of the single mode fiber, which contributes to a relatively low splicing loss between the optimized dual-core photonic crystal fiber and the single mode fiber. The calculations results show that the total loss induced by the similar mode field radius and numerical aperture is as low as about 0.026 dB, less than that between the traditional photonic crystal fiber and single mode fiber of 0.1 dB. The performance of the hydrostatic pressure sensor based on the optimized dual-core photonic crystal fiber with a length of 20 cm was studied, and the results show the sensitivity is about -1.6 pm/MPa in the range from 0 to 500 MPa.

Key words: Fiber optics; Hydrostatic pressure sensing; Finite element method; Dual-core photonic crystal fibers; Mode field radius; Numerical aperture

OCIS Codes: 060.5295; 060.2370; 230.2285; 120.5475; 130.6010

0 Introduction

Hydrostatic pressure measurement is necessary in a variety of areas[1]. Varieties of specialty fibers, including polymer optical fibers[2-4], high-doped fibers[2] and photonic crystal fibers[4-6], offer new possibilities to enhance sensing measurement sensitivity for pressure detection. Photonic Crystal Fibers (PCFs)[7], which also are called microstructured optical fiber, have been investigated since they appeared in the mid 1990s due to their superior properties in single mode transmission[8], large negative

Foundation item: The National High Technology Research and Development Program of China (No. 2013AA031501), the Projects of Zhejiang Province (Nos. 2010R50007, 2011C21038, 2011R10065), the Program for Science and Technology Innovative Research Team in Zhejiang Normal University.

First author: LI Hai-tao (1988-), male, M.S. degree candidate, mainly focuses on fiber sensing technology. Email:1822093874@qq.com

Supervisor (Corresponding author): CHEN Da-ru (1982-), male, professor, Ph.D. degree, mainly focuses on fiber sensing and fiber laser. Email:daru@zjnu.cn

Received: Dec. 8, 2016; **Accepted**: Mar. 17, 2017

dispersion[9-10], highly birefringence[11-13], non-linearity[14] and so on. The unique advantages of PCFs make them very promising in many sensing applications. Various types of PCF sensors with excellent performances have already been proposed, such as pressure sensor[15], strain sensor[16], refractive index sensor[17-18]. Among them, the sensing of hydrostatic pressure based on PCFs[25-27] has also attracts considerable attention recently. Since the previously reported pressure sensor[15] is not compact due to a Sagnac interferometer formed by a long PCF and an optical coupler, we proposed a relatively compact sensor which was based on a novel Designed Dual-core Photonic Crystal Fiber (DC-PCF)[22-24]. The reported 10 cm DC-PCF can be used as a hydrostatic pressure sensor[19-21] due to the pressure sensitive mode coupling of the two fiber cores of the DC-PCF. Unfortunately, the distance of the two fiber cores of the DC-PCF is less than 4 μm and the fiber core is much smaller than the Single Mode Fiber (SMF) which results in the difficulty of the splicing due to the relatively large gap of the mode field radius (M_s) and the numerical aperture (N_r) between the DC-PCF and the conventional SMF.

In this paper, based on our previous work, a novel DC-PCF that can match well with the conventional SMF is proposed. In the cross-section of the proposed DC-PCF, each of the two solid fiber cores can be seen as the missing two layers of air holes in the triangular lattice instead of the missing one air hole for previously proposed DC-PCF. By adjusting the structure parameters of the novel DC-PCF, we have the optimal values 10.09 μm and 0.139 for M_s and the N_r respectively. The optimized DC-PCF we proposed here matches well with the conventional SMF with the mode field radius and numerical aperture of 10 μm and 0.14, respectively, which results in a low splicing loss. Further more, we presented the one-to-one correspondence between the hydrostatic pressure applied on the DC-PCF and the peak wavelength shift of the transmission spectrum.

1 Structure and simulation method

The proposed DC-PCF with a cross-section shown in Fig. 1(a) is formed by a triangular lattice of circular air holes with two solid cores separated by one air hole. Each of the two solid fiber cores can be seen as missing two layers of air holes in the triangular lattice. Fig. 1(b) shows the enlarged view of one fiber core which is marked as the circle in the Fig. 1(a). The hole pitch of the triangular lattice is Λ and the diameter of the small air hole is $2r$ in the cross-section of the proposed DC-PCF. The refractive index of the air is assumed to be 1.0 and the refractive index of the fused silica is 1.444 at 1550 nm according to the well-known Sellmeier equation

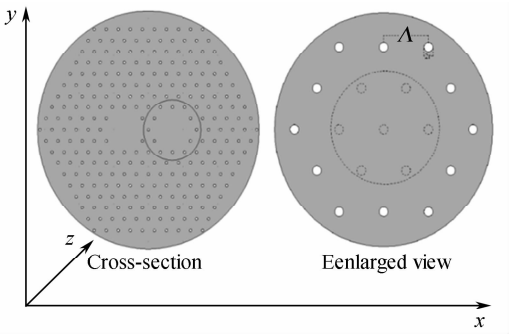

Fig. 1 Cross-sectionand enlarged view of the fiber core of the proposed DC-PCF

$$n^2(\lambda) = 1 + \frac{B_1\lambda^2}{\lambda^2 - C_1} + \frac{B_2\lambda^2}{\lambda^2 - C_2} + \frac{B_3\lambda^2}{\lambda^2 - C_3} \tag{1}$$

where n is the refractive index, λ is the wavelength, $B_{1,2,3}$ and $C_{1,2,3}$ are experimentally determined Sellmeier coefficients. Note that this λ is the vacuum wavelength.

A full-vector Finite-Element Method (FEM) is used to investigate the guided modes of the proposed DC-PCF. The DC-PCF under the pressure will result in pressure induced refractive index change according to the well-known photoelastic effect. The changing of pressure-induced refractive index of the silica under the hydrostatic pressure are given by the equations as[19]

$$\Delta n_x = n_x - n_0 = -C_1\sigma_x - C_2(\sigma_y + \sigma_z) \tag{2}$$

$$\Delta n_y = n_y - n_0 = -C_1\sigma_y - C_2(\sigma_x + \sigma_z) \tag{3}$$

$$\Delta n_z = n_z - n_0 = -C_1\sigma_z - C_2(\sigma_x + \sigma_y) \tag{4}$$

where σ_x, σ_y and σ_z are the stress components, $C_1 = 6.5\times10^{-13}$ m^2/N and $C_2 = 4.2\times10^{-12}$ m^2/N are the stress-optic coefficients of pure silica, where x-axis parallels the any side of regular hexagon in the Fig. 1 (a), and y-axis perpendiculars to x-axis and it also in the cross-section of the proposed DC-PCF, and z-axis

follows the direction of the air hole. For the DC-PCF under the pressure, the stress components of the silica can be achieved based on the FEM analysis of the optical fiber under the hydrostatic pressure.

As we previously reported the hydrostatic pressure sensor based on a DC-PCF, the pressure-induced refractive index change of the DC-PCF results in the wavelength peak shift of the transmission spectrum when the light is injected into one fiber core of the DC-PCF due to the mode coupling of the two fiber cores. According to the mode coupling theory, the optical power transferred from one fiber core to the other fiber core after a length Z along the fiber we proposed based on mode coupling theory is given by

$$p(\lambda,Z) = \sin(|n_e - n_o| Z \cdot \pi/\lambda) = \sin^2(\Delta n_{eo} Z \cdot \pi/\lambda) \tag{5}$$

where n_e, n_o are the calculated effective refractive indices of the even mode and odd mode, respectively. Thus, we can calculate the transmission spectrum from one fiber core of the novel DC-PCF with a fixed length according to Eq. (5).

2 Properties and performance

2.1 Normalized electric field distribution

Fig. 2 shows the normalized electric field distribution along the radial x-direction of the SMF, the novel DC-PCF and the previous proposed DC-PCF, which are achieved by using the FEM to investigate the guided modes. As we all know, the SMF has one fiber core with a diameter of 8.3 μm, which is much larger than the previously proposed DC-PCF with a normalized electric field distribution mark as the green curve. However, the novel DC-PCF shows a similar normalized electric field distribution as the SMF, which will contribute to reducing the power loss in the splicing interface between the PCF and the SMF. Inset shows the mode profile of the SMF, the novel DC-PCF and the previous proposed DC-PCF respectively. Note that only one fiber core of the DC-PCF is described here and the parameters of the calculated novel DC-PCF (previous DC-PCF) are r=0.34 μm, Λ=3.48 μm (r=0.7 μm, Λ=2 μm).

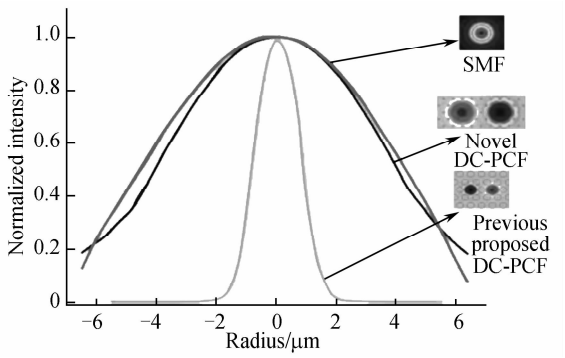

Fig. 2 Electric field distribution of SMF, novel DC-PCF and previous proposed DC-PCF

2.2 Mode field radius and numerical aperture

The M_s and the N_r play an important role in the splicing loss between the PCF and the SMF. The insert loss (L_{il}) induced by the N_r mismatch is given by

$$L_{il} = 10\log\frac{(N_{as})}{(N_{ar})} \tag{6}$$

where N_{as} and N_{ar} are the numerical aperture of transmitting and receiving optical fiber respectively. The formula indicates that the insert loss can be reduced by using two fibers with similar numerical aperture. The insert loss (L_{il}) caused by the mismatch of mode field radius can be expressed by

$$L_{il} = 20\log\frac{w_r^2 + w_s^2}{2w_r w_s} \tag{7}$$

where w_s and w_r are the mode field radius of transmitting and receiving optical fiber respectively. The formula indicates that the insert loss may reach the lowest by using two fibers with similar mode field radius. Firstly, we try to optimize the M_s and the N_r of our previously reported DC-PCF by adjusting the structure parameters. The cross-section of the earlier DC-PCF is formed by a triangular lattice of circular air holes with two missing air holes as two fiber cores which are separated from one air hole. Now, we have to design a novel DC-PCF with different structures. The small air holes are still arranged by following the principle of a triangular lattice. The only difference is that the region of the fiber core can be seen as missing two layers of air holes, as Fig. 1 shows.

We also investigate the change rules of the M_s and the N_r of this novel DC-PCF, which is shown in Fig. 3. We can see the novel DC-PCF follows the similar rules as the previous DC-PCF does. Based on the

above conclusion, we try to design an optimized DC-PCF which has the lowest splicing loss. Fig. 4 shows the total insert loss of the novel DC-PCFs which is caused by the mismatch of the M_s and the N_r with different structure parameters. We can find that each curve has a minimum value in the calculated range which means there is an optimized structure parameter combination. Our calculations shows that when we choose $\Lambda=3.48$ μm, $r=0.34$ μm $r=0.34$ μm, as the structure parameters of the optimized DC-PCF, the total splicing loss is only about 0.026 dB which is acceptable since the splicing loss for the SMF to SMF is usually about 0.1 dB when using a commercial fiber splicer. The optimized DC-PCF has the M_s of 10.09 μm and the N_r of 0.139, respectively.

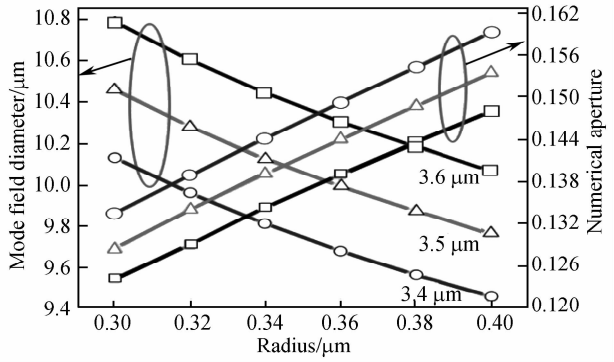

Fig. 3 Mode field diameter and numerical aperture with different parameters of the novel DC-PCF

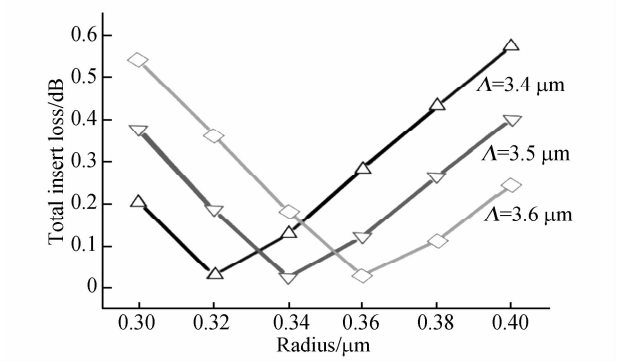

Fig. 4 Total insert loss with different hole radius and hole pitch

2.3 Hydrostatic pressure sensor

Finally the performance of the hydrostatic pressure sensor based on this optimized DC-PCF has been investigated. Fig. 5(a) shows the (x-polarized) transmission spectrum of the DC-PCF with a length of 20 cm at hydrostatic pressure of 0, 100, 200, 300, 400 and 500 MPa. There is a one-to-one correspondence between the pressure and the output spectrum for the optimized DC-PCF based pressure sensor, when we focus on the peak wavelength λ_p λ_p rang from 1530 nm to 1580 nm. We can achieve the relationship between the peak wavelength and hydrostatic pressure, which comes out to be a linear relationship as shown in Fig. 5(b). The calculation shows that the sensitivity of the optimized DC-PCF based pressure sensor is about −1.6 pm/MPa.

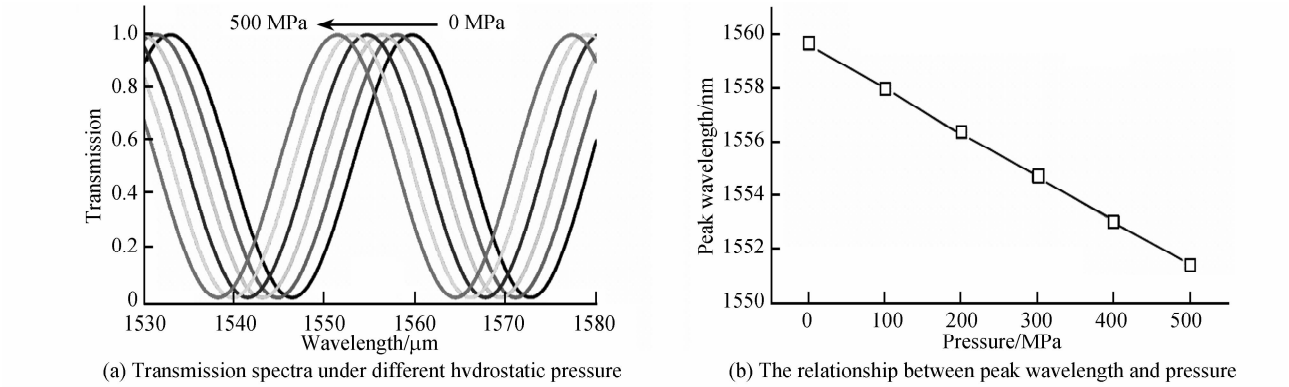

Fig. 5 Transmission spectra and peak wavelength (around 1550 nm) of the transmission spectra of a 20-cm optimized DC-PCF versus hydrostatic pressure

3 Conclusion

In conclusion, we have proposed and investigated a novel DC-PCF with well matched the M_s and the N_r with the SMF in the application of hydrostatic pressure sensing. The fiber cores of the novel DC-PCF is formed from missing two layers of air holes instead of missing one air hole, which contributes to achieving the same M_s and N_r as that of the SMF. The M_s and the N_r of the proposed DC-PCF dependent on the structure parameters have been investigated. The significant advantage of this novel DC-PCF is that it can match well with the conventional SMF, resulting in a low splicing loss caused by the M_s mismatch and the

N_r mismatch. By adjusting the hole radius and the hole pitch, we obtained the optimized DC-PCF with the splicing loss about 0.026 dB for the M_s mismatch and the N_r mismatch. Finally, the performance of the hydrostatic sensor based on the optimized DC-PCF has been investigated.

References

[1] JR M, ORMSBEE A. An introduction to fluid dynamics[M]. Cambridge University Press, 2000.

[2] JIN L, QUAN Z, CHENG L, *et al*. Hydrostatic pressure measurement with heterodyning fiber grating lasers: mechanism and sensitivity enhancement[J]. *Journal of Lightwave Technology*, 2013, **31**(9): 1488-1494.

[3] FAVERO F, QUINTERO S, MARTELLI C, *et al*. Hydrostatic pressure sensing with high birefringence photonic crystal fibers[J]. *Sensors*, 2010, **10**(11): 9698-9711.

[4] MARTYNKIEN T, WOJCIK G, MERGO P, *et al*. Highly birefringent polymer side-hole fiber for hydrostatic pressure sensing[J]. *Optics Letters*, 2015, **40**(13): 3033-3036.

[5] SZCZUROWSKI M, MARTYNKIEN T, STATKIEWICZ-BARABACH G, *et al*. Measurements of polarimetric sensitivity to hydrostatic pressure, strain and temperature in birefringent dual-core microstructured polymer fiber[J]. *Optics Express*, 2010, **18**(12): 12076-12087.

[6] TARNOWSKI K, ANUSZKIEWICZ A, OLSZEWSKI J, *et al*. Nonlinear frequency conversion in a birefringent microstructured fiber tuned by externally applied hydrostatic pressure[J]. *Optics Letters*, 2013, **38**(24): 5260-5263.

[7] KNIGHT J. Photonic crystal fibres[J]. *Nature*, 2003, **424**(6950): 847-851.

[8] BIRKS T, KNIGHT J, RUSSELL P. Endlessly single-mode photonic crystal fiber[J]. *Optics Letters*, 1997, **22**(13): 961-963.

[9] HUTTUNEN A, TORMA P. Optimization of dual-core and microstructure fiber geometries for dispersion compensation and large mode area[J]. *Optics Express*, 2005, **13**(2): 627-635.

[10] YANG Si-gang, ZHANG Ye-jin, PENG Xiao-zhou, *et al*. Theoretical study and experimental fabrication of high negative dispersion photonic crystal fiber with large area mode field[J]. *Optics Express*, 2006, **14**(7): 3015-3023.

[11] CHEN Da-ru, SHEN Lin-fang. Highly birefringent elliptical-hole photonic crystal fibers with double defect[J]. *Journal of Lightwave Technology*, 2007, **25**(9): 2700-2705.

[12] BELTRAN-MEJIA F, CHESINI G, SILVESTRE E, *et al*. Ultrahigh-birefringent squeezed lattice photonic crystal fiber with rotated elliptical air holes[J]. *Optics Letters*, 2010, **35**(4): 544-546.

[13] CHEN Da-ru, WU G. Highly birefringent photonic crystal fiber based on a double-hole unit[J]. *Applied Optics*, 2010, **49**(9): 1682-1686.

[14] KNIGHT J, SKRYABIN D. Nonlinear waveguide optics and photonic crystal fibers[J]. *Optics Express*, 2007, **15**(23): 15365-15376.

[15] FU H, TAM H, SHAO Li-yang, *et al*. Pressure sensor realized with polarization-maintaining photonic crystal fiber-based Sagnac interferometer[J]. *Applied Optics*, 2008, **47**(15): 2835-2839.

[16] DONG Xin-yong, TAM H, SHUM P. Temperature-insensitive strain sensor with polarization-maintaining photonic crystal fiber based Sagnac interferometer[J]. *Applied Physics Letters*, 2007, **90**(15): 151113.

[17] TOWN G, YUAN W, MCCOSKER R, *et al*. Microstructured optical fiber refractive index sensor[J]. *Optics Letters*, 2010, **35**(6): 856-858.

[18] YUAN W, TOWN G, BANG O. Refractive index sensing in an all-solid twin-core photonic bandgap fiber[J]. *IEEE Sensors Journal*, 2010, **10**(7): 1192-1199.

[19] WU Chuang, GUAN B, WANG Zhi, *et al*. Characterization of pressure response of bragg gratings in grapefruit microstructured fibers[J]. *Journal of Lightwave Technology*, 2010, **28**(9): 1392-1397.

[20] CHEN Da-ru, HU Gu-feng, CHEN Ling-xia. Dual-core photonic crystal fiber for hydrostatic pressure sensing[J]. *IEEE Photonics Technology Letters*, 2011, **23**(24): 1851-1853.

[21] LIU Zheng-yong, TSE M, WU Chuang, *et al*. Intermodal coupling of supermodes in a twin-core photonic crystal fiber and its application as a pressure sensor[J]. *Optics Express*, 2012, **20**(19): 21749-21757.

[22] REVATHI S, INABATHINI S, PAL J. Pressure and temperature sensor based on a dual core photonic quasi-crystal fiber[J]. *Optik*, 2015, **126**(22): 3395-3399.

[23] CAI Shi-wei, YU Song, WANG Yu-huang, *et al*. Hybrid dual-core photonic crystal fiber for spatial mode conversion [J]. *IEEE Photonics Technology Letters*, 2016, **28**(3): 339-342.

[24] HE Hui-mei, WANG Li, YIN Li-dan, *et al*. Transverse load sensing based on a dual-core photonic crystal fiber[J]. *Optik - International Journal for Light and Electron Optics*, 2015, **126**(23): 4574-4576.

[25] HU Gu-feng, CHEN Da-ru. Side-hole dual-core photonic crystal fiber for hydrostatic pressure sensing[J]. *Journal of Lightwave Technology*, 2012, **30**(14): 2382-2387.

[26] HU Gu-feng, CHEN Da-ru, JIANG Xiao-gang. Side-hole two-core microstructured optical fiber for hydrostatic pressure sensing[J]. *Applied Optics*, 2012, **51**(20): 4867-4872.

[27] CHEN Da-ru, HU Gu-feng, TSE M, *et al*. Design of a dual-core dual-hole fiber for hydrostatic pressure sensing[J]. *Optics Communications*, 2012, **285**(10-11): 2615-2619.